

# Detection of Iron Emission Line from the Galaxy Cluster Including the Radio Galaxy 3C220.1 at $z = 0.62$

Naomi Ota (ota@astro.isas.ac.jp)<sup>1</sup>,

Kazuhisa Mitsuda (mitsuda@astro.isas.ac.jp)<sup>1</sup>,

Makoto Hattori (hattori@astr.tohoku.ac.jp)<sup>2</sup>,

and

Tatehiro Mihara (mihara@crcosmo.riken.go.jp)<sup>3</sup>

Received \_\_\_\_\_; accepted \_\_\_\_\_

---

<sup>1</sup>Institute of Space and Astronautical Science, 3-1-1 Yoshinodai, Sagamihara, Kanagawa, 229-8510, Japan

<sup>2</sup>Astronomical Institute, Tōhoku University, Aoba, Sendai, 980-8578, Japan

<sup>3</sup>Institute of Physical and Chemical Research, 2-1 Hirosawa, Wako, Saitama, 351-0198, Japan

## ABSTRACT

We have detected an emission line feature at 4 keV in the X-ray emission from a sky region including the distant radio galaxy 3C220.1 ( $z = 0.62$ ) obtained with ASCA. The line energy is 6.1 – 7.0 keV (90% confidence) in the rest frame of 3C220.1. Within the present statistics, the observed spectra are consistent with two different models: a non-thermal model consisting of a power-law continuum plus a 6.4 keV iron emission line, and a Raymond-Smith thin-thermal emission model of  $kT \sim 6$  keV with a metal abundance of  $\sim 0.5$  solar. However, because of the large ( $\sim 500$  eV) equivalent width of the line, a significant fraction of the X-ray emission is likely to arise from the hot intracluster gas associated with the galaxy cluster that includes 3C220.1. The spectral parameters of the thermal emission are consistent with the luminosity-temperature relation of nearby clusters.

*Subject headings:* Galaxies:Clusters:Individual (3C220.1) – X-Rays:Galaxies – Cosmology:Gravitational Lensing

## 1. Introduction

Among a variety of attempts searching for clusters at high redshifts, X-ray observation directly illuminates the gravitational potential well because the X-ray-emitting hot plasma is considered to trace it. Moreover, X-ray emission lines from highly ionized ions, iron in particular, can be used to determine the redshift of the hot gas, and thereby its association with other objects can be investigated. Based on these ideas we have conducted an observation of the radio galaxy 3C220.1 with ASCA.

The existence of a galaxy cluster which surrounds the radio galaxy 3C220.1 ( $z = 0.62$ ) was first suggested from the observations at Lick Observatory (Dickinson 1984). Around the radio galaxy in the Lick image, several quite red galaxies were found. Further observations were performed at Kitt Peak National Observatory, and the blue band image revealed the presence of a giant luminous arc (Dickinson 1984). In 1995, much higher quality images were obtained with the Hubble Space Telescope (Dickinson 1998). A large arc (9 arc seconds in radius and subtending  $\sim 70$  degrees around the radio galaxy) was clearly resolved.

The arc image of 3C220.1 is regarded as a section of an Einstein ring caused by gravitational lensing. This offers a remarkable tool to constrain the cluster mass enclosed within it. The redshift of the arc was successfully determined using the Keck telescope to be  $z_s = 1.49$  (Dickinson 1998). Under an assumption of spherically symmetric geometry, the projected lensing mass within the arc radius,  $9''$ , is  $M_{\text{lens}}(< 9'') = 3.8 \times 10^{13} M_{\odot}$ . Here  $\Omega_0 = 1$ ,  $\Lambda = 0$ , and  $H_0 = 50 \text{ km s}^{-1} \text{ Mpc}^{-1}$  are adopted. The derived mass is appropriate for clusters of galaxies rather than a single galaxy.

A strong evidence for the existence of a galaxy cluster around 3C220.1 was obtained by the X-ray observation with ROSAT observatory (Hardcastle *et al.* 1998). The ROSAT HRI image revealed that the the X-ray emission consists of a compact central component and an extended component which can be attributed to cluster emission. The ratio of the count

rates of the compact to the extended components in ROSAT HRI energy band is about 2 to 3.

In this paper we report the detection of an iron-K emission line with ASCA and discuss the origin of the X-ray emission.

## 2. OBSERVATION AND RESULTS

### 2.1. Observation

We observed 3C220.1 with the ASCA GIS and SIS for 40 ksec on 1998 April 11, during the AO6 period. The GIS was operated in the PH nominal mode, while the SIS was in the Faint 1CCD mode. The data were filtered by the standard ASCA data screening procedure.

X-ray emission centered at  $(9^{\text{h}}32^{\text{m}}43^{\text{s}}, +79^{\text{d}}06^{\text{m}}39^{\text{s}})_{\text{J2000.0}}$  is detected. The peak position is about 0.2 arcmin off from the cataloged value of 3C220.1 but is consistent with it within the uncertainty of ASCA attitude determinations (0.5 arcmin at 90% confidence). The source count rates are  $(6.6 \pm 0.4) \times 10^{-3}$  counts/sec in the 0.7 – 8 keV band for the GIS and  $(8.6 \pm 0.5) \times 10^{-3}$  counts/sec in the 0.5 – 8 keV for the SIS within a circle of 3' radius centered on the peak position, after background subtraction. In the GIS and SIS fields, there are several other bright sources in the vicinity of 3C220.1. Most of them are not identified with known objects, except for one at  $(9^{\text{h}}31^{\text{m}}34^{\text{s}}, +79^{\text{d}}04^{\text{m}}9^{\text{s}})_{\text{J2000.0}}$  which is a radio-loud AGN (see comments in Hardcastle *et al.* 1998).

### 2.2. Spectral Analysis

Since the angular separations between 3C220.1 and the three of nearby sources are 3.4 to 5.1 arcmin, the contamination of 3C220.1's energy spectrum from these sources must be

carefully treated. In order to check the contribution due to the nearby sources, we have accumulated the energy spectra in two different integration regions: (1) a circular region centered at 3C220.1 with a radius of 3.0 arcmin and (2) the same circular region as (1) but excluding three circular areas centered on the nearby sources. The radii of the excluded regions are proportional to the intensity of the nearby sources. We then evaluated these two spectra by model-fittings. For both power-law and Raymond-Smith models, the resultant model parameters for the different extraction regions are consistent with each other within the statistical errors. In what follows, we show the results for case (1) because at present only the azimuthally averaged response function is available for the X-ray telescope; thus case (2) may involve some systematic errors.

The PHA (Pulse Height Analysis) channels of the spectra were first converted to PI (Pulse Invariant) channels and the spectra of the two telescopes of the same system, i.e. SIS-0 and 1, and GIS-2 and 3, respectively, were added together. Some of the PI bins are combined together so that the number of counts in any combined PI bin is greater than 30.

We subtracted background spectra estimated in two different ways and compared the results in order to estimate systematic errors. In the first case (a), the spectrum was estimated from the present observation. For the GIS background, we accumulated events from annular image regions whose centers are at the optical axes of the telescopes. The outer and inner radii are respectively equal to the maximum and minimum angular distances of the target spectrum region from the optical axis. We excluded regions 4 arcmin from the target and the contaminating sources. While for the SIS background, image regions were selected outside 4 arcmin from the target and  $\sim 3$  arcmin from the contaminating sources. In the other case (b), the standard background spectrum which was obtained through blank sky-field observations during the ASCA PV phase was used. The background was derived from the same detector region as the target on the SIS/GIS detector coordinates. The

systematic errors of background originate from spatial fluctuations of the Cosmic X-ray Background, the detector-position dependence of Cosmic X-ray Background and non-X-ray background, and temporal variation of non-X-ray background. Their contribution to the above two backgrounds are different. However, the spectral fits using the different backgrounds provided consistent results within the statistical errors. Thus the systematic errors are smaller than Poisson statistical errors. Since the statistical errors of parameters using (b) are smaller than those using (a) by 30 – 50 %, we will show the results obtained with (b) hereafter.

We fitted the GIS and SIS spectra simultaneously with model spectra. First we tried a simple single component model; a single power-law model with neutral absorption with a column density fixed at the Galactic value,  $N_{\text{H}} = 1.93 \times 10^{20} \text{ cm}^{-2}$  (Stark *et al.* 1992). The absorption is fixed at this value throughout this paper. The fits are acceptable with a best-fit power-law photon index of 1.9 (1.7 – 2.0, 90% error); however, the fit leaves two excess data points at around 4 keV for both the SIS and GIS spectra (Figure 1).

EDITOR: PLACE FIGURE 1 HERE.

The deviations of the data from the model in the 3.2 – 4.3 keV band are only 0.2 to  $2.1\sigma$  (Here  $\sigma$  stands for a standard deviation). However, the probability that we should observe such deviations in any corresponding consecutive energy bins of two different detectors is encouragingly low,  $\sim 0.5\%$ . We thus added a narrow Gaussian emission line to the model with the Gaussian center energy left free. The result is shown in Table 1 and Figure 1. In comparison to the single power-law model fit, the fit improves from a  $\chi^2$  value of 33.9 for 34 degrees of freedom to 26.5 for 32 degrees of freedom. The improvement is significant by the F-test at the 98.1% confidence level. Thus we conclude that the emission line feature is significant at the 98.1% confidence level.

The best-fit Gaussian center energy is 3.9 keV in our frame with the 90% error range of 3.8 – 4.2 keV. The most likely origin of this line feature is a red-shifted iron emission line. If we assume low-ionization iron emission lines at 6.4 keV, the redshift is estimated to be 0.63 (0.53 – 0.69, 90% error), while if we assume 6.7 keV lines from helium-like iron, the redshift is 0.71 (0.61 – 0.76). Therefore the redshift of the radio galaxy ( $z = 0.62$ ) is within the error range in either case. Thus it is most likely that the emission is originating from 3C220.1 or cluster surrounding it. Then the central energy is estimated to be 6.3 (6.1 – 7.0) keV in the rest frame. It can be interpreted either as a 6.4 keV low-ionization iron emission line which may be associated with AGN, 6.7/6.9 keV lines from highly ionized irons which may be attributed to cluster hot gas, or a combination of these two. We are not able to distinguish these emission lines under the current limited statistics and detector resolutions.

Thus, we next performed fits with models corresponding to the above two extreme cases: a power-law model plus a Gaussian emission line with the line center energy fixed at 6.4 keV, and a Raymond-Smith model representing an optically thin thermal plasma emission. We fixed the redshift value at the position of the radio galaxy, 0.62. The results of these fits are shown in Figure 2 and Table 2, where the model parameters for the GIS and SIS spectrum are combined. Although both models are acceptable at the 90% confidence limit, the Raymond-Smith model gives a smaller reduced  $\chi^2$  value. The luminosity in the 2 – 10 keV band is  $1 \times 10^{45}$  erg/s, assuming a distance of  $z = 0.62$ .

For the non-thermal model consisting of a power-law plus a 6.4keV line, we obtained an equivalent width of  $\sim 500$  (190 – 780) eV, while for the Raymond-Smith fit, we found a metal abundance of 0.54 (0.17 – 1.0) solar. In Figure 3 we have plotted the  $\chi^2$  contours as a function of two of the Raymond-Smith model parameters:  $kT$  and metal abundance.

EDITOR: PLACE FIGURE 2 HERE.

EDITOR: PLACE FIGURE 3 HERE.

### 3. DISCUSSION

We have detected an emission line at 3.9 keV (3.8 – 4.2 keV) in our rest frame, which corresponds to 6.1 – 7.0 keV at  $z = 0.62$ . Within the present statistics, the observed spectra are consistent with two different models; a non-thermal model which consists of a power-law continuum and a 6.4 keV emission line, and a Raymond-Smith thermal model with temperature about 6 keV. In this section, we discuss the origin of the X-ray emission.

The radio source 3C220.1 is classified as an FR II narrow emission line galaxy (NELG). Turner *et al.* (1997) investigated the narrow iron K line at 6.4 keV from type 2 AGNs systematically, and reported that most of the NELG show an equivalent width smaller than 200 eV and on average  $\sim 100$  eV. Thus for 3C220.1, the derived equivalent width under a non-thermal model is a factor of 2 to 8 larger than the typical NELGs if one attributes all of the line intensity to the radio galaxy 3C220.1. This indicates a large ( $> 50\%$ ) fraction of the iron line is emitted from the other emission region: most likely the intracluster medium in the galaxy cluster.

The ROSAT HRI observations revealed that the X-ray emission consists of a compact component and an extended component which is significantly extended more than 10 arcsec in radius and carries about 60% of the HRI photons (Hardcastle *et al.* 1998). Since the two spectral models in our analysis are not distinguished within the statistics, any combination of the two models should also be statistically acceptable. If the compact component carries 40% of the photons in the ASCA energy band and contains an iron emission line of 100 eV equivalent width in its own spectrum, the equivalent width of the rest of the emission is expected to be 250 eV to 1200 eV. This value is appropriate for thin thermal emission of



$kT \sim 6$  keV with a metal abundance of 0.2 to 1.6 solar.

If we consider about 60% of the total emission to arise from the cluster, the luminosity and the temperature obtained from the spectral fit are consistent with the luminosity-temperature relation for nearby clusters obtained by David *et al.* (1993) within the scatter of data points.

The masses of distant clusters determined from the gravitational arc (lens mass) and determined from the X-ray observations (X-ray mass) have been compared by several authors (e.g. Wu & Fang 1997). These results show that in general the X-ray mass is either consistent with or smaller than the lens mass. Under the assumption of hydrostatic equilibrium, isothermal and spherical distribution of the intracluster gas, and  $\beta$ -model surface brightness distribution, the X-ray mass projected within a radius  $r$  is estimated as  $M_{x\beta}(r) = (3kT\beta/G\bar{m})(\pi/2)(r^2/\sqrt{r^2 + r_c^2})$ , where  $k$  is Boltzmann constant and  $\bar{m}$  is the mean mass per plasma particle (Ota *et al.* 1998). Adopting the best-fit  $\beta$ -model parameters obtained from the ROSAT HRI observations ( $\beta = 0.9$  and the core radius,  $r_c = 13''$ ), we find that the X-ray mass contained within the arc radius is equal to or smaller than the lens mass if the temperature of the X-ray emission is lower than 6.4 keV. The determined X-ray temperature of  $5.6_{-1.1}^{+1.5}$  keV from the single Raymond-Smith model fits is consistent with this.

In conclusion, a large fraction of the iron line emission and the continuum emission associated with the line is likely to originate from the intracluster medium in the galaxy cluster around 3C220.1. This is strong evidence for the existence of a cluster of galaxies including 3C220.1.

We are very grateful to M. Dickinson for valuable information and discussions on the recent HST results and also to D.M. Worrall for sending us the ROSAT results before

publication. We would like to thank D. Audley for his careful review of the manuscript. This work was supported in part by the Japan Society for the Promotion of Science.

## REFERENCES

- David, L. P., Slyz, A., Jones, C., Forman, W., & Vrtillek, S. D., 1993, *ApJ*, 412, 479.
- Dickinson, M., 1984, Ph.D. thesis, University of California.
- Dickinson, M., 1998, private communication.
- Fort, B., & Mellier, Y., 1994, *A&A Rev.*, 5, 239.
- Hardcastle, M. J., Lawrence, C. R., & Worrall, D. M., 1998, *ApJ*, 504, 743.
- Ota, N., Mitsuda, K., & Fukazawa, Y., 1998, *ApJ*, 495, 170.
- Stark, A. A., Gammie, C. F., Wilson, R. W., Bally, J., Linke, R.A., Heiles, C., & Hurwitz, M., 1992, *ApJS*, 79, 77.
- Turner, T. J., George, I. M., Nandra, K. & Mushotzky, R. F., 1997, *ApJS*, 113, 23.
- Wu, Z-P. & Fang, L-Z, 1997, *ApJ*, 483, 62.

## Figure Captions

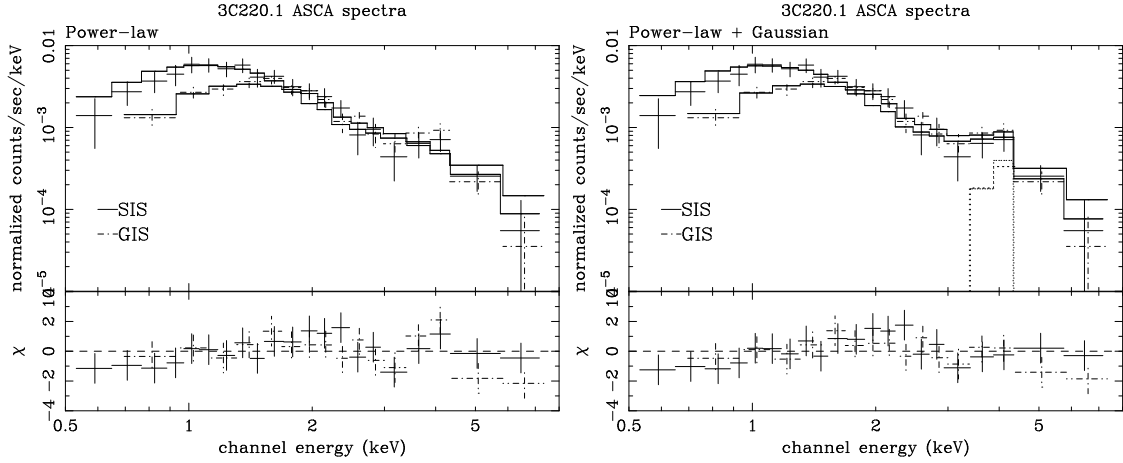


Fig. 1.— Spectral fits of ASCA SIS(0+1) and GIS(2+3) spectra with a power-law model (left panel) and a power-law plus a Gaussian model (right panel). The crosses denote the observed spectra and the step functions show the best-fit model function convolved with the X-ray telescope and the detector response functions. In the right panel, the Gaussian component is shown with the dotted line.

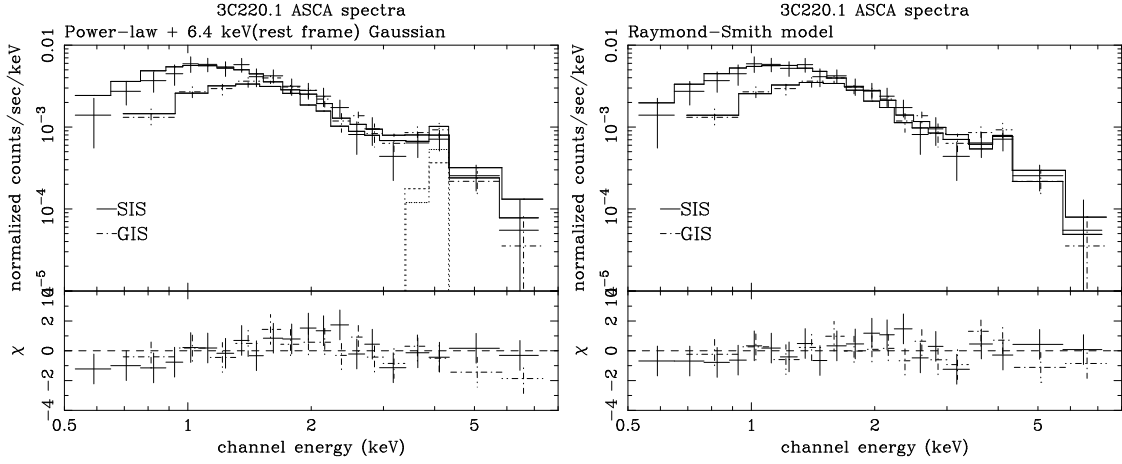


Fig. 2.— Spectral fits of ASCA SIS(0+1) and GIS(2+3) spectra with a power-law plus 6.4 keV (rest-frame) Gaussian model (left panel), and with a Raymond-Smith model (right panel). The redshift of the object is assumed to be 0.62. In the left panel, the Gaussian component is shown with the dotted line.

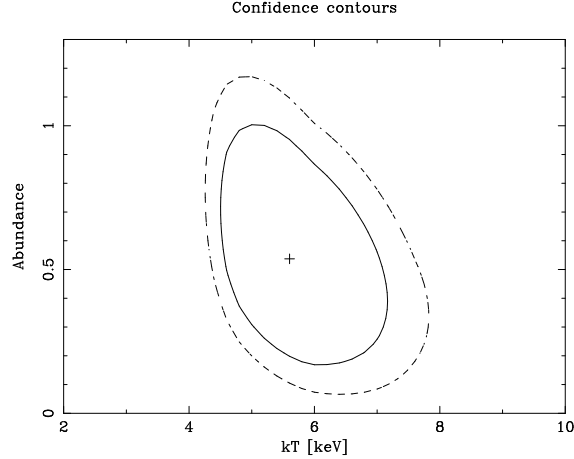


Fig. 3.—  $\chi^2$  contours of the Raymond-Smith fit. The 90% single-parameter and two-parameter error domains are shown as contours with solid and broken curves, respectively. The position of the  $\chi^2$  minimum is denoted with a cross.

Table 1: Results of Spectral Fits

Model	Parameter	Value ( error <sup>†</sup> )
Power-law	Photon Index	1.9 (1.8 – 2.1)
	$\chi^2/\text{d.o.f}$	33.9/34
Power-law plus Gaussian	Photon Index	1.9 (1.8 – 2.1)
	Gaussian Center Energy [keV]	3.9 (3.8 – 4.2)
	$\chi^2/\text{d.o.f}$	26.5/32

---

The absorption column density was fixed at the Galactic value;  $N_{\text{H}} = 1.93 \times 10^{20} [\text{cm}^{-2}]$ .

The sigma value of the Gaussian functions is fixed at 0.03 keV.

<sup>†</sup>The quoted errors correspond to a single parameter error at 90% confidence.

Table 2: Results of Spectral Fits

Model	Parameter	Value ( error*)
Power-law plus Gaussian	Normalizaion <sup>†</sup>	1.3 (1.1 – 1.4)
	Photon Index	1.9 (1.8 – 2.1)
	Equivalent width [eV] <sup>‡</sup>	480 (190 – 780)
	$\chi^2/\text{d.o.f}$	26.7/33
	$L_X^{2-10}$ [erg/s] <sup>♣</sup>	$1.1 \times 10^{45}$
Raymond-Smith	Normalizaion <sup>†</sup>	9.4 (8.1 – 10.7)
	kT[keV]	5.6 (4.5 – 7.1)
	Abundance [ $Z_\odot$ ]	0.54 (0.17 – 1.0)
	$\chi^2/\text{d.o.f}$	18.1/33
	$L_X^{2-10}$ [erg/s] <sup>♣</sup>	$1.0 \times 10^{45}$

The absorption column density was fixed at the Galactic value;  $N_H = 1.93 \times 10^{20} [\text{cm}^{-2}]$ .

\*The quoted errors correspond to a single parameter error at 90% confidence.

<sup>†</sup>Flux at 1keV (in  $10^{-4}$  photons  $\text{s}^{-1}\text{keV}^{-1} \text{cm}^{-2}$ ) for the power-law fit or  $\int n_e n_h dV / 4\pi D^2$  (in  $10^{-18} \text{cm}^{-5}$ ) for the Raymond-Smith fit, where  $D$  is the distance to the source (cm),  $n_e$  and  $n_h$  are the electron and hydrogen densities ( $\text{cm}^{-3}$ ) .

<sup>‡</sup>A narrow line at 6.4 keV is assumed.

<sup>♣</sup>Absorption-corrected 2 – 10 keV luminosity assuming a distance corresponding to  $z = 0.62$ .